

Russell K. Monson · Jed P. Sparks · Todd N. Rosenstiel
Laura E. Scott-Denton · Travis E. Huxman
Peter C. Harley · Andrew A. Turnipseed
Sean P. Burns · Brant Backlund · Jia Hu

Climatic influences on net ecosystem CO₂ exchange during the transition from wintertime carbon source to springtime carbon sink in a high-elevation, subalpine forest

Received: 15 February 2005 / Accepted: 18 May 2005 / Published online: 10 August 2005
© Springer-Verlag 2005

Abstract The transition between wintertime net carbon loss and springtime net carbon assimilation has an important role in controlling the annual rate of carbon uptake in coniferous forest ecosystems. We studied the contributions of springtime carbon assimilation to the total annual rate of carbon uptake and the processes involved in the winter-to-spring transition across a range of scales from ecosystem CO₂ fluxes to chloroplast photochemistry in a coniferous, subalpine forest. We observed numerous initiations and reversals in the recovery of photosynthetic CO₂ uptake during the initial phase of springtime recovery in response to the passage of alternating warm- and cold-weather systems. Full recovery of ecosystem carbon uptake, whereby the 24-h cumulative sum of NEE (NEE_{daily}) was consistently negative, did not occur until 3–4 weeks after the first signs of photosynthetic recovery. A key event that preceded full recovery

was the occurrence of isothermality in the vertical profile of snow temperature across the snow pack; thus, providing consistent daytime percolation of melted snow water through the snow pack. Interannual variation in the cumulative annual NEE (NEE_{annual}) was mostly explained by variation in NEE during the snow-melt period (NEE_{snow-melt}), not variation in NEE during the snow-free part of the growing season (NEE_{snow-free}). NEE_{snow-melt} was highest in those years when the snow melt occurred later in the spring, leading us to conclude that in this ecosystem, years with earlier springs are characterized by lower rates of NEE_{annual}, a conclusion that contrasts with those from past studies in deciduous forest ecosystems. Using studies on isolated branches we showed that the recovery of photosynthesis occurred through a series of coordinated physiological and biochemical events. Increasing air temperatures initiated recovery through the upregulation of PSII electron transport caused in part by disengagement of thermal energy dissipation by the carotenoid, zeaxanthin. The availability of liquid water permitted a slightly slower recovery phase involving increased stomatal conductance. The most rate-limiting step in the recovery process was an increase in the capacity for the needles to use intercellular CO₂, presumably due to slow recovery of Rubisco activity. Interspecific differences were observed in the timing of photosynthetic recovery for the dominant tree species. The results of our study provide (1) a context for springtime CO₂ uptake within the broader perspective of the annual carbon budget in this subalpine forest, and (2) a mechanistic explanation across a range of scales for the coupling between springtime climate and the carbon cycle of high-elevation coniferous forest ecosystems.

Communicated by Jim Ehleringer

R. K. Monson (✉) · J. P. Sparks · T. N. Rosenstiel
L. E. Scott-Denton · T. E. Huxman · P. C. Harley
A. A. Turnipseed · S. P. Burns · B. Backlund · J. Hu
Department of Ecology and Evolutionary Biology,
University of Colorado, Boulder, CO 80309-0334, USA
E-mail: Russell.Monson@colorado.edu
Tel.: +1-303-4926319
Fax: +1-303-4928699

R. K. Monson
Cooperative Institute for Research in Environmental Science,
University of Colorado, Boulder, CO 80309, USA

P. C. Harley · A. A. Turnipseed · S. P. Burns
National Center for Atmospheric Research,
Boulder, CO 80301, USA

Present address: J. P. Sparks
Department of Ecology and Evolutionary Biology,
Cornell University, Ithaca, NY, USA

Present address: T. E. Huxman
Department of Ecology and Evolutionary Biology,
University of Arizona, Tucson, AZ 85721-0088, USA

Keywords Conifers · AmeriFlux · Rocky Mountains · Eddy · Turbulent · Fir · Pine · Spruce · Hydrology · Carboxylation efficiency · Quantum Yield · Chlorophyll fluorescence · Xanthophyll

Introduction

Climate transitions between the winter and spring exert a principal control over the photosynthetic dynamics of coniferous forest ecosystems (Troeng and Linder 1982; Leverenz and Öquist 1987; Lundmark et al. 1998; Law et al. 2000; Lloyd et al. 2002; Monson et al. 2002; Huxman et al. 2003; Tanja et al. 2003; Ensminger et al. 2004). One of the advantages of the evergreen coniferous growth form is the rapid upregulation of photosynthetic activities during the spring warm-up, which allows trees to capitalize quickly on favorable weather conditions. This “quick start” extends the length of the growing season and minimizes the canopy developmental constraint to seasonal photosynthesis that is often exhibited by deciduous trees (e.g., Goulden et al. 1996b; Black et al. 2000; Barr et al. 2002). Despite the obvious advantage of rapid springtime recovery in coniferous trees, and a significant volume of research on the biochemical and biophysical processes involved in the springtime upregulation of photosynthesis (see Öquist and Huner 2003 for a review), only limited insight has been uncovered about the influence of the springtime recovery on the annual rate of ecosystem carbon uptake and the coupling of the recovery process to transitions in specific climate variables.

Air and soil temperatures have been most widely cited as the dominant controls over springtime photosynthetic recovery. In northern Sweden, Bergh and Linder (1999) used beneath-soil heating cables to demonstrate that soil temperature had a key role in triggering the seasonal recovery. Tanja et al. (2003) used a statistical analysis of site-to-site variation in the timing of spring CO₂ uptake to deduce that air temperature had a primary role in triggering photosynthetic recovery in boreal forests in Finland, while beneath-snow soil temperature had no significant role. In a study of the effects of spring air temperatures on the photochemical components of photosynthesis in Scots pine trees in central Siberia, Ensminger et al. (2004) found that warm weather triggers rapid upregulation of photosynthesis, but that subsequent cold weather can reverse the photosynthetic cues. Thus, there is growing consensus that air temperature is a primary cue that regulates seasonal switches in the carbon cycling of coniferous forests from cold climates.

Studies of the components of the photosynthetic apparatus that respond to increases in air temperature have focused on the photochemical processes (see Öquist and Huner 2003). Ottander and Öquist (1991) studied several pine species and reported that photosynthetic quantum yields were low at the end of winter, but recovered within 3 days when trees or branches were transferred to a warm laboratory setting. Verhoeven et al. (1996, 1998, 1999) have shown that wintertime downregulation of photosynthesis in a number of different species involves sustained engagement of xanthophyll-cycle energy dissipation from photosystem II (PSII), and that in two coniferous species from cold

montane environments, the recoveries of PSII and the xanthophyll cycle occur within a few days after warming. Ensminger et al. (2004) have shown that in Scots pine needles during winter, downregulation of photosynthesis is accompanied by similar changes in the xanthophyll-cycle, as well as reductions in the amount of total chlorophyll, D1 protein of the PSII reaction center, and PSII light harvesting complexes. In late spring, with the onset of warmer air temperatures, Ensminger et al. (2004) observed recovery of PSII activity, increased levels of chloroplast protein synthesis, and rearrangements of pigment complexes. Insight into the springtime recovery of other components of the photosynthetic apparatus (e.g., stomatal conductance, Rubisco activity) remains rudimentary. Past studies have shown that the full recovery of CO₂ assimilation and stomatal conductance is dependent on soil thaw, warm air temperatures and adequate water uptake (Smith 1985; Jurik et al. 1988; Day et al. 1989), but the timing of this recovery in relation to the natural seasonal transition of ecosystem CO₂ exchange, and its relationship to the recovery of the photochemical components of photosynthesis, has yet to be determined.

We report the results from a 5-year study in a subalpine coniferous forest in the Rocky Mountains of Colorado, USA. We aim to provide greater insight into the importance of springtime net ecosystem CO₂ exchange (NEE) to the overall, annual rate of NEE, and identify the mechanisms that force the transition in the forest from being a wintertime CO₂ source to a springtime CO₂ sink. Our observations span the range from ecosystem CO₂ flux to chloroplast photochemistry and focus on four specific issues: (1) the difficulties surrounding a precise definition of the time of transition from winter net ecosystem CO₂ loss to spring net ecosystem CO₂ gain (i.e. the forest ‘turn-on date’), (2) the quantitative relationship between interannual variation in the rate of carbon uptake during spring snow melt and interannual variation in the rate of total annual carbon uptake, (3) the environmental variables that are most important in triggering the forest turn-on date, and (4) the physiological processes that are most limiting to the springtime upregulation of photosynthetic CO₂ assimilation. This insight has relevance to not only the suite of biochemical and physiological adaptations that have evolved in these trees, but also to the potential for future climate warming to shift the seasonal transition in CO₂ exchange, and thus influence dynamics in the global carbon cycle.

Materials and methods

The study site

The studies were conducted at the Niwot Ridge AmeriFlux site located at 3,050 m above sea level in a subalpine forest just below the Continental Divide near Nederland, Colorado (40° 1′ 58″N; 105° 32′ 47″W). The

secondary forest surrounding the site is ~ 100 years old, having regrown after early twentieth-century logging. The forest is dominated by subalpine fir (*Abies lasiocarpa*, 46% of the mean tree density), Engelmann spruce (*Picea engelmannii*, 28% of the mean tree density), and lodgepole pine (*Pinus contorta*, 26% of the mean tree density). The understory is relatively sparse, containing tree seedlings from all three species and patches of *Vaccinium myrtillus* (25% average understory coverage). The forest slopes gently (6–7%) and uniformly, decreasing from west to east. Maximum (late-summer) leaf area index (LAI) for the forest is estimated to be $4.2 \text{ m}^2 \text{ m}^{-2}$, canopy gap fraction is 17%, canopy height is 11.4 m, displacement height is 7.6 m, and roughness length is 1.79 m. Annual precipitation for the site averages 800 mm (approximately 65% falling as snow) and the mean annual temperature is 1.5°C . General characteristics of turbulent fluxes of CO_2 , H_2O and sensible heat were reported in Turnipseed et al. (2003, 2004) and energy budget characteristics were reported in Turnipseed et al. (2002). Overall dynamics in forest carbon uptake have been previously reported for 1999 and 2000 in Monson et al. (2002).

Eddy covariance measurements

Turbulent fluxes were measured at 21.5 m from a scaffolding-type tower. Details of the flux measurements have been reported previously (Monson et al. 2002; Turnipseed et al. 2002, 2003, 2004). Briefly, the eddy covariance method was used to measure the eddy flux for CO_2 , H_2O and temperature (see Baldocchi 2003 for a review of the eddy covariance method). Wind velocity was measured with a 3-dimensional sonic anemometer (model CSAT-3, Campbell Scientific, Logan) and CO_2 concentration was measured with a closed-path infrared gas analyzer (model 6262, LiCor, Inc., Lincoln). Density corrections due to changes in H_2O vapor concentrations were made according to Webb et al. (1980). Wind coordinates were rotated according to Kaimal and Finnigan (1994) for the data of 1999–2001, and according to Wilczak et al. (2001) for the data of 2002–2003, to force the mean crosswind and vertical wind speeds to zero. We have conducted extensive analyses of these coordinate rotation methods at our site, compared them to other rotation methods, and estimated potential errors in the calculated eddy flux due to low-frequency filtering, all of which is reported in a previous publication (Turnipseed et al. 2003). The storage of CO_2 within the canopy was measured using a vertical profile system as described in Monson et al. (2002). The change in stored CO_2 was added to the calculated eddy flux of CO_2 to provide net ecosystem CO_2 exchange (NEE) as described by Goulden et al. (1996a). By convention, NEE is considered negative in sign when the net CO_2 flux is from the atmosphere to the forest and positive when the net flux is from the forest to the atmosphere.

Soil and snow measurements

Soil temperatures were measured using cross-calibrated, copper-constantan thermocouples for a single level (5 cm) in the soil and platinum resistance thermometers with integrated temperature for the upper 10 cm of the soil. Soil moisture was measured using water content reflectometers (model CS615, Campbell Scientific, Logan). The probes were inserted so as to measure the integrated soil moisture in the top 15 cm of soil. Snow temperature profiles were made in one of two ways; manually (2001) by digging a snow pit and using a handheld copper-constantan thermocouple inserted into the undisturbed wall of the pit (~ 10 cm) at different heights or automatically (2002) using one 100-cm and two 200-cm long polycarbonate wands (model TP101, Measurement Research Corporation, Gig Harbor), with thermistors (accuracy of $\pm 0.1^\circ\text{C}$ from -40 to 80°C) embedded at 10-cm intervals and connected to dataloggers (model CR10, Campbell Scientific, Logan). When deployed in the field, the lower 20 cm of each wand was buried in the soil during the summer and left in place during the winter. As snow buried the wands, the vertical profile in snow temperature, at 10-cm intervals, was obtained. We evaluated the snow-temperature profile only using thermistor readings that were located between, and including, the nearest thermistor to 10-cm below the upper snow surface and 10-cm above the ground surface, in order to avoid boundary effects due to solar heating from above or ground heating from below. Calibration of the wands against a precision mercury thermometer was accomplished in the laboratory, prior to installation in the field, using a controlled-temperature water bath. All of the climatic, snow and soil measurements were made within a 30×30 m plot located approximately 50 m northwest of the eddy covariance tower.

Branch-level experiments

We conducted two different branch-level experiments to study the recovery of photosynthetic capacity after transfer from the cold wintertime condition to a warmer and/or hydrated springtime condition. One experiment was conducted during the third week of March, 2000 (Experiment 1) and one was conducted during the first week of April, 2004 (Experiment 2). In Experiment 1, branches from four adult lodgepole pine trees were collected in the field (diameter at breast height > 15 cm), at mid-canopy on March 15, 2000. Greater than 1 m of snow fell on the study site during the week immediately prior to the branch collections. All branches were harvested before dawn, needle water potentials (Ψ_w) and chlorophyll fluorescence patterns were measured (see below for methods) in an instrument trailer located at the site, and needles were collected for later pigment analysis. Branches were then transported (total transit time of 1 h) in opaque plastic bags kept on ice to

laboratory facilities at the University of Colorado, Boulder. One branch from each of the four trees was randomly placed into one of the following treatments: (1) low light with no hydration (referred to as low-light dry or LLD) with a 14 h photoperiod and a photosynthetic (400–700 nm) photon flux density (PPFD) of $10 \mu\text{mol m}^{-2} \text{s}^{-1}$ at 25°C ; (2) low light with photoperiod and temperature as above, but stems were re-cut under tap water and the cut end was placed in tap water for further hydration (referred to as low-light, hydrated or LLH), and (3) temperature as above and hydration as above, but kept under high light in a glasshouse (maximum PPFD of $1,800 \mu\text{mol m}^{-2} \text{s}^{-1}$) and natural photoperiod (approximately 12.4 h) supplemented with artificial light from metal-halide lamps to produce a total photoperiod of 14 h (referred to as high-light, hydrated or HLH). Branches were randomly chosen from the treatments for sampling of physiological and biochemical traits over the subsequent 5 days of recovery.

In Experiment#2, branches from subalpine fir and lodgepole pine trees were harvested before dawn on March 31, 2004 from trees with diameter at breast height >15 cm at mid-canopy height. In this case, the week prior to the harvest was characterized by warmer-than-normal temperatures (mean temperature of 2.7°C compared to $-2.1 \pm 0.8^\circ\text{C}$ for this same week during the previous 5 years). Needles were immediately measured for Ψ_w and fluorescence, and transported to the laboratory, as described above. Once at the laboratory, the branches were placed into one of four different treatments: (1) a warm growth chamber (model E-15, Conviron, Inc., Toronto) ($20/15^\circ\text{C}$ day/night, $300 \mu\text{mol m}^{-2} \text{s}^{-1}$ PPFD, 14-h photoperiod) without subsequent re-hydration (referred to as warm, dry or WD), (2) a cold growth chamber ($1.5/0.5^\circ\text{C}$ day/night, $300 \mu\text{mol m}^{-2} \text{s}^{-1}$, 14 h photoperiod) without subsequent re-hydration (referred to as cold, dry or CD), (3) the same warm growth chamber described above, but with re-hydration (referred to as warm, wet or WW), and (4) the same cold growth chamber described above, but with re-hydration (referred to as cold, wet or CW). Once again, branches were randomly chosen from the treatments for measurement, in this case during a subsequent 7-day recovery period.

Branch and needle measurements

Needle water potentials were determined using a Scholander-type pressure chamber (PMS Inc, Corvallis) with N_2 as the pressurization gas. Stomatal conductance (g_s) was measured with an open-flow gas exchange system (model 6400, LiCor Inc., Lincoln). Chamber temperature was held at 25°C and relative humidity was maintained between 20–40%. All measurements were made with saturating light (PPFD = $1,500 \mu\text{mol m}^{-2} \text{s}^{-1}$; model LS-2 halogen light source, Hansatech, King's Lynn) using the factory-provided conifer cuvette system. Five measurements of gas-exchange were made and averaged

over a one-minute period after the cuvette conditions had stabilized. Total needle surface area was determined for each experimental branch using the volume displacement method described by Chen et al. (1997).

The relationship between net CO_2 assimilation rate (A) and the intercellular CO_2 concentration (C_i) (referred to as the $A-C_i$ response) was initiated at ambient CO_2 concentration ($365 \mu\text{mol mol}^{-1}$). Chamber CO_2 concentration (C_a) was then reduced to $200 \mu\text{mol mol}^{-1}$ for 5 min to stimulate stomatal opening. Assimilation rate was determined at this value, then C_a was reduced to $75 \mu\text{mol mol}^{-1}$, followed by incremental increases to 150, 250, 350, 550, 700, 800, 900, 1200, and $2000 \mu\text{mol mol}^{-1}$. The data from the $A-C_i$ responses were analyzed using Photosynthesis Assistant (Dundee Scientific Ver. 1.1.2; Dundee) and photosynthetic parameters (e.g., $V_{C_{\text{max}}}$, J_{max} , R_d , TPU) were calculated as in Harley et al. (1992).

Chlorophyll fluorescence emissions were measured using a portable pulse amplitude-modulated fluorometer (model PAM-2000, Walz, Effeltrich) as described in Demmig-Adams et al. (1996). In all treatments, needles were briefly dark adapted (5 min) before determining the intrinsic PSII efficiency, calculated as F_v/F_m (the ratio of variable fluorescence to maximum fluorescence). Needles to be used in pigment analysis were frozen in liquid nitrogen, freeze-dried, and stored under a N_2 atmosphere at -80°C until processing. Chlorophylls and carotenoids were extracted according to Adams and Demmig-Adams (1992) and analyzed using the HPLC column and gradient system described by Gilmore and Yamamoto (1991).

Statistical analysis

Differences among means for the branch-level recovery experiment were evaluated using repeated measures ANOVA. In cases where interactions among variables were not of interest, we used repeated measures one-way ANOVA. In this case, we tested for significant differences among measurement means for each species independently at different times during the experiment or for differences between species at specific times. In cases where interactions among variables were of interest, we used a repeated measures, three-way, split-plot, ANOVA, in this case testing for the significance of time, recovery treatment type, and their interaction. To evaluate the $A-C_i$ response, data were compared across treatments and time by the use of non-linear regression of the gas exchange data (Huxman et al. 1998). The non-linear regression model (Jacob et al. 1995) was fit through the complete data set (all times and treatments), then individually (each treatment and time point separately) and F -statistics were constructed from the residual sum of squares from each regression line following Potvin et al. (1990). In comparing mean values of photosynthesis rate and photosystem II efficiency in branches of fir and pine allowed to recover for 7 days in a

cold regime or warm regime (i.e., in Table 4 last two columns for each species), we used the Student's *t*-test for independent samples. Linear and non-linear regression analyses were conducted using the Regression Wizard found in SigmaPlot ver. 6.10 (SPSS, Inc). Significance of regression models was tested using ANOVA. We tested all regressions for normality of residuals using the Kolmogorov-Smirnov test and constancy of variance using the Levene Median test at $P < 0.05$. In the analysis of the relationship between daytime mean NEE and daytime mean temperature (i.e., reported in Table 2), not all regressions passed these tests. We have decided to report the regressions, nonetheless, with appropriate notation of which tests were failed, for two reasons: (1) because the ANOVA used to test for the significance of regressions is robust with regard to failure of these tests (Pedhazur 1997), and (2) our purpose in presenting the regressions is not to develop specific models of variable dependence, but rather to heuristically probe the potential for variable relationships at different times of the year.

In those analyses involving the calculation of daily, seasonal or annual cumulative NEE, we used flux data that included gap-filled values. This was required because cumulative data is sensitive to the total number of summed intervals. In these cases, we used data from all "flag" categories, with gap-filling accomplished as described in the Niwot Ridge AmeriFlux data archive (http://urquell.colorado.edu/data_ameriflux/). In those analyses where we assessed 30-min averaged NEE as a function of temperature or season (i.e., Figs. 1, 4, 5, Table 2) we eliminated flux data from the analysis that had been derived from the various gap-filling procedures. This means that we only used flux values that had been flagged with the value "1" in the Niwot Ridge AmeriFlux data record. In those cases, the inclusion of gap-filled data would have compromised the analysis as many of the "filled data" are derived from the relationship between NEE and temperature, the same relationship being probed in the analyses. Averaged data is not sensitive to the total number of averaged intervals, facilitating our decision to use only non gap-filled data.

Results

Date of transition from CO₂ source to CO₂ sink and duration of spring snow melt

Although we observed evidence of daytime, 30-min averaged NEE values ($NEE_{30\text{-min}}$) that were negative in sign (reflecting apparent net CO₂ uptake) throughout the winter, these observations were infrequent, positively correlated to air temperature, and relatively small in magnitude until the month of April; all of which suggests that these values did not reflect photosynthetic recovery. For example, during the mid-winter months of January and February negative NEE values were observed for only 16% of the total non gap-filled, 30-min

averaging periods across all 5 years. Of those negative $NEE_{30\text{-min}}$ that were observed in January and February across all 5 years, 69% were near zero (i.e., between 0 and $-0.5 \mu\text{mol m}^{-2} \text{s}^{-1}$). A significant correlation was observed between negative $NEE_{30\text{-min}}$ values in January and February (pooled across all 5 years) and air temperature ($y = 0.081x - 6.33$, $R^2 = 0.01$, $F = 20.42$; $df = 1,525$; $P < 0.0001$). However, this correlation was positive in sign, indicating that as air temperature increased, $NEE_{30\text{-min}}$ values became less negative, not more negative; this reflects a response of respiration to temperature, not photosynthesis. It is possible that the complex topography of the site and non-ideal wind flow patterns result in small errors in the $NEE_{30\text{-min}}$ during certain winter conditions. However, the low frequency of these observations, their low magnitude and the positive correlation with air temperature indicate that they probably do not reflect true photosynthetic recovery.

In Fig. 1, we present the five-year averaged pattern of the transition in $NEE_{30\text{-min}}$ during the winter and spring for the purpose of illustrating general trends in the transition. As will become evident in later sections, there is considerable interannual variance around the mean pattern shown in Fig. 1. Wintertime average $NEE_{30\text{-min}}$ was always positive in sign, whether averaged for daytime or nighttime periods (Fig. 1). The nighttime-averaged $NEE_{30\text{-min}}$ increased slightly as the seasons progressed but, clearly, most of the seasonal change occurred in the daytime $NEE_{30\text{-min}}$, indicative of photosynthetic recovery. During the second or third week of April daytime-averaged $NEE_{30\text{-min}}$ switched from being slightly higher to slightly lower than nighttime-averaged $NEE_{30\text{-min}}$ (marked by arrow#1 in Fig. 1). This switch reflected the first time during the spring when daytime

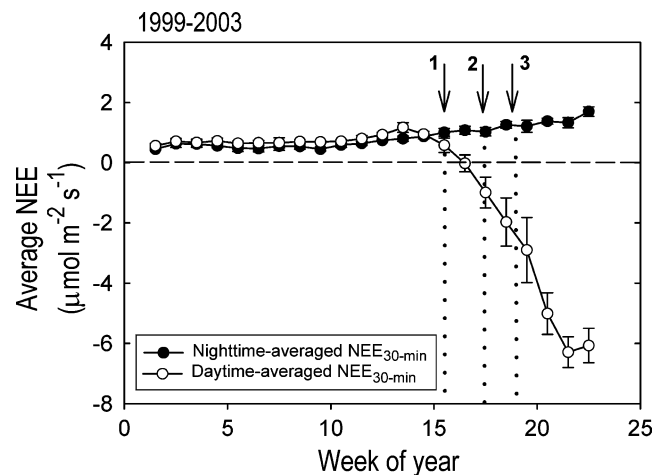


Fig. 1 Weekly average $NEE_{30\text{-min}}$ during the day (0600–1730 h) or night (1800–0530 h) for the five-year observation period. The data included in this analysis was the "raw", non-gap-filled, 30-min NEE averaged data. Vertical bars represent ± 1 S.E. The arrows#1,#2 and#3 mark reference points that are discussed in the text. It should be noted that arrow#3 reflects the point at which the daily cumulative NEE became negative; given the cumulative nature of this calculation it was made using gap-filled data

periods of net photosynthetic CO₂ uptake were of high enough magnitude and frequency to offset the late-spring bias toward slightly higher ecosystem respiration rates during the day, compared to the night. The switch is presumably a response to the slow warming of springtime conditions. Even after this switch, however, daytime rates of NEE_{30-min} that reflect net CO₂ uptake were relatively weak in magnitude and not consistent in their frequency of occurrence; in fact, the daytime-averaged NEE_{30-min} remained positive in sign at the time of the switch. Within 1 or 2 weeks after this initial switch, we observed a date when daytime NEE_{30-min} values were consistently negative in sign (reflecting net CO₂ uptake) and relatively consistent in frequency of occurrence and magnitude (we used the un-averaged data from this analysis to apply the arbitrary metric that NEE_{30-min} had to be $< -3 \mu\text{mol m}^{-2} \text{s}^{-1}$ for at least three consecutive half-hour averaging periods for at least three consecutive days) (marked by arrow#2 in Fig. 1). Finally, within 1 or 2 weeks following this second step in forest recovery, we observed the first day when the daily (24-h) cumulative NEE (NEE_{daily}) switched from being positive in sign to being consistently negative in sign (we used the NEE_{30-min} data to create 24-h averages for this analysis) (marked by arrow#3 in Fig. 1). Thus, the time of photosynthetic recovery (reflected in arrows#1 or#2, depending on how one defines “recovery”), occurs well before the time of ecosystem carbon balance recovery (reflected in arrow#3). Among the 5 years, we found the length of time between photosynthetic recovery (taken as arrow#2 in Fig. 1) and ecosystem carbon balance recovery (taken as arrow#3 in Fig. 1) to consistently be 9–11 days (significant correlation between the two variables; $R^2 = 0.80$, $F = 11.70$; $df = 1,3$; $P = 0.042$). Clearly, there are several possible ways to define the date of springtime photosynthetic recovery. From this point forward, we will refer to the ‘forest turn-on date’ as the date of recovery in ecosystem carbon balance; i.e. that date when NEE_{daily} first became consistently negative in sign (i.e. arrow#3 in Fig. 1).

Measurements of daily cumulative net ecosystem CO₂ exchange during the spring snow melt

The length of the “snow melt period” (time from the forest turn-on date to the date when diurnal fluctuations in soil temperature indicated disappearance of the snow pack) each spring was variable among years (Table 1). At one extreme, the entire snow melt lasted only 6 days following the forest turn-on in 2002. This was the year with the shallowest spring snow pack recorded for this site in over 50 years of continuous measurements (<http://culter.colorado.edu/Niwot/NiwotRidgeData/C1.html>), and resulted in completely snow-free conditions by the end of April. At the other extreme, the snow melt persisted for 36 days following the forest turn-on in 1999, a year with a deeper-than-average spring snow pack. During 1999, a 55% increase in the snow pack was observed for

the late-spring month of April alone (Table 1, Column 4), and the snow melt period lasted well into the month of June.

Cumulative NEE during the snow melt period (NEE_{snow-melt}, defined as the sum of NEE_{daily} between the date when NEE_{daily} first switched to negative values and the end of snow melt) ranged from 3% to 42% of the total growing-season NEE [defined as NEE_{snow-melt} plus the cumulative NEE during the snow-free part of the growing season (NEE_{snow-free})] (Table 1). Despite being confined to a shorter time interval (6–36 days), the interannual range of NEE_{snow-melt} (7.7 mol m^{-2}) was over two times the range of NEE_{snow-free} (3.5 mol m^{-2}), despite the latter lasting several months longer. Year-to-year variation in the length of the snow-free part of the growing season was determined more by variation in the length of snow melt in the spring (which varied by a total of 30 days), than variation in the date of growing season closure in the fall (which varied by a total of 13 days, see Table 1 footnote “g”). Cumulative wintertime NEE (NEE_{winter}) exhibited the least amount of variation from year to year, with the total range of variation being only 2.6 mol m^{-2} . The amount of cumulative warming (degree-days) from February 1 to the first day of photosynthetic recovery (arrow # 2 in Fig. 1) varied among years, whether assessed above a threshold of 0°C or 5°C (Table 1). There was no common temperature threshold among years leading up to the first day of photosynthetic recovery.

The timing and magnitude of NEE_{daily} during the snow melt period was variable among the 5 years, with the greatest rates of CO₂ uptake (i.e., the steepest slope to the cumulative NEE_{daily} as a function of date) occurring during those years with the latest snow melt (Fig. 2). During 2001, an extended (5-day) cold-weather system moved into the site immediately following the forest turn-on date, causing the slope of the relationship between NEE_{daily} and date to flatten out and even reverse itself as several days during this period exhibited net CO₂ loss. NEE during the snow melt was dependent on air temperature whether expressed as NEE_{daily} (which contains gap-filled data) or NEE_{30-min} (which does not contain gap-filled data) (Figs. 3a, b). Nonlinear regression analysis revealed a best-fit polynomial function to both sets of data ($y = ax^2 + bx + c$; $a = 1.49$, $b = -26.15$, $c = -100.28$; $R^2 = 0.43$; $F = 42.81$; $df = 2,114$; $P < 0.0001$ for NEE_{daily}, and $y = ax^2 + bx + c$; $a = 0.291$, $b = -0.695$, $c = -3.68$; $R^2 = 0.29$; $F = 22.33$; $df = 2,110$; $P < 0.0001$ for NEE_{30-min}). Non-linear regression models explained slightly more variance in both data sets than linear models (data not shown). NEE_{daily} became less negative at daily mean air temperatures below 5°C and above 10°C (Figs. 3a, b). The mean air temperature observed during the spring snow melt was higher during years when the initiation of snow melt and, concomitantly, the forest turn-on date occurred later in the spring (Fig. 3c); although this relationship could not be statistically validated given the limited number of observations ($y = 0.141x - 12.40$, $R^2 = 0.51$, $F = 3.19$; $df = 1,3$; $P = 0.17$).

Table 1 Springtime climate, snow and cumulative NEE data for the Niwot Ridge AmeriFlux site during five consecutive years

| Year ^a | Spring snow duration (days) ^b | SWE (cm) ^c | Δ SWE (%) ^d | Mean annual temperature (°C) ^e | Snow-melt NEE (mol C m ⁻²) ^f | Snow-melt (NEE _{snow-melt}) (mol C m ⁻²) ^g | Snow-free NEE (NEE _{snow-free}) (mol C m ⁻²) ^h | Winter NEE (NEE _{winter}) (mol C m ⁻²) ^h | Annual NEE (NEE _{annual}) (mol C m ⁻²) ⁱ | Springtime percentage of growing season NEE (%) ^j | Degree days > 0°C to first date of midday net CO ₂ uptake ^k | Degree days > 5°C to first date of midday net CO ₂ uptake ^k |
|-------------------|--|-----------------------|-------------------------------|---|---|---|---|---|---|--|---|---|
| 1999 | 36 | 36.2 | +55 | 1.9 ± 0.1 | -8.03 | -10.89 | 12.21 | -6.71 | 42 | 42 | 81 | 33 |
| 2000 | 27 | 31.4 | -38 | 3.5 ± 0.1 | -3.51 | -13.31 | 12.02 | -4.80 | 21 | 21 | 54 | 22 |
| 2001 | 26 | 25.4 | -9 | 2.3 ± 0.1 | -3.35 | -13.73 | 11.44 | -5.64 | 20 | 20 | 67 | 41 |
| 2002 | 6 | 19.2 | -100 | 2.4 ± 0.1 | -0.33 | -10.38 | 9.58 | -1.13 | 3 | 3 | 68 | 32 |
| 2003 | 28 | 42.6 | -14 | 2.6 ± 0.1 | -5.10 | -10.22 | 10.07 | -5.05 | 33 | 33 | 89 | 49 |

^aThe period in any one year used for measurement of net ecosystem CO₂ exchange (NEE) in this study spans from November 1 – October 31. Thus, the first date of the NEE time series began on November 1, 1998

^bThe length of springtime snow cover determined as the time between the first date when NEE_{daily} was negative and the date when the combination of soil temperature and soil heat flux measurements revealed a snow-free surface (see Figs. 4, 5 for examples of the sudden rise in soil temperature at the time of snow melt)

^cThe maximum annual snow-water equivalent measured during the spring of each year. The long-term (1988–1998) mean maximum SWE is 46.3 ± 5.6 cm (range = 25.4–88.9 cm)

^dThe percentage change in the SWE between March 31 and April 30. This value is included to indicate the tendency for snow to appear or disappear from the snowpack during the critical spring month of April

^eMean annual temperature at 21.5 m height for the period between November 1 and October 31 each year. Values are mean ± S.E. of the annual 30-min temperature means. The long-term (1952–2000) mean annual temperature is 1.5 ± 0.2°C for this site

^fThe cumulative (cum) NEE for the forest during the snowmelt period taken from the first date during the spring that NEE_{daily} exhibited a negative value to the date the combination of soil temperature and soil heat flux measurements revealed a snow-free surface

^gThe cumulative (cum) NEE for the forest during the snow free part of the growing season determined as the time between the first spring date when the combination of soil temperature and soil heat flux measurements indicated a snow-free surface and the first autumn date when NEE_{daily} was positive in value (DOY 289, 300, 296, 296, 287 for 1999, 2000, 2001, 2002, 2003, respectively)

^hThe cumulative (cum) NEE for the forest from the first autumnal date when NEE_{daily} was positive to the first spring date when NEE_{daily} was negative

ⁱThe total annual cumulative (cum) NEE for the entire year designated as in “a” above

^jThe value in column 6 (“f”) as a fraction of (column 6 + column 7) (“f” + “g”)

^kThe number of cumulative degree days above 0°C or 5°C for the period from February 1 to the first date when midday NEE_{30-min} was < -3 μmol m⁻² s⁻¹ for 3 consecutive averaging periods for 3 consecutive days; this arbitrarily chosen threshold was assumed to be driven primarily by changes in gross photosynthesis rate and thus reflect a physiologically-relevant response to cumulative warming

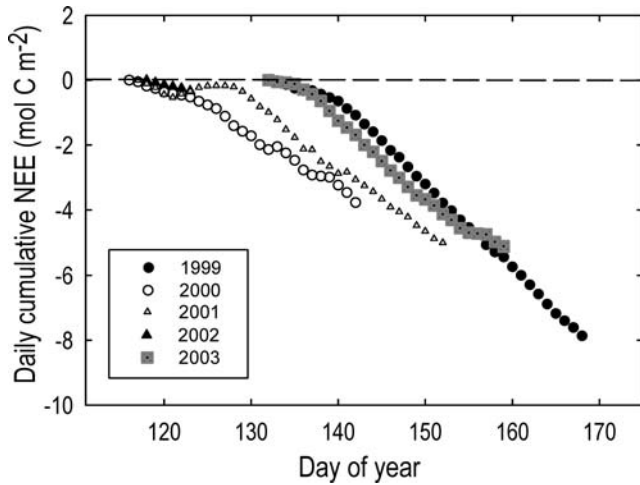


Fig. 2 Cumulative daily NEE (NEE_{daily}) for the period during the spring snow melt during five successive years at the Niwot Ridge AmeriFlux site. The time period of snow melt was determined as described in Table 1. The day of year (DOY) for the initiation of NEE_{daily} was 134, 116, 117, 118 and 132, for 1999, 2000, 2001, 2002 and 2003, respectively

Temperature had a greater effect on photosynthetic recovery as the season progressed from winter toward spring. We analyzed the degree of statistical correlation between mean daily air temperature and NEE_{30-min} during the binned periods between January 1 and March 1 (mid-winter), during the 3-week period just prior to the forest turn-on each year, and during the period of snow melt following the forest turn-on date (Table 2). We found no correlation between NEE_{30-min} and air temperature during the mid-winter months for any of the 5 years of observation. During the 3-week period just prior to the forest turn-on date, a significant correlation was present during all five years. We also observed significant correlations between NEE_{30-min} and air temperature during the snow melt period for 4 of the 5 years of observation. The one year that did not exhibit a significant correlation was the snowmelt period for 2002 which, once again, was characterized by only 6 days.

In order to gain insight into interannual variation in the coupling between springtime climate and the forest turn-on date, we conducted detailed studies during the spring snow melt for two (2001 and 2002) of the five years of observation. In the spring of 2001, the forest turn-on date was defined as DOY 117. Three periods of brief warm weather occurred earlier in the spring (marked by a, b, and c in Fig. 4a), which coincided with small, but unsustainable amounts of forest CO_2 uptake (marked by a, b, and c in Fig. 4d). A few days after the forest turn-on date, a cold-weather system moved into the site and lasted for 5 days (marked by d in Fig. 4a). We were not able to successfully measure eddy fluxes of CO_2 during 4 out of the 5 days in this period due to a power outage (thus the gap in the NEE data of Fig. 4d marked by d), but as evidenced in the successful measurements on the last day, the forest turn-on was probably reversed during this period, and the ecosystem

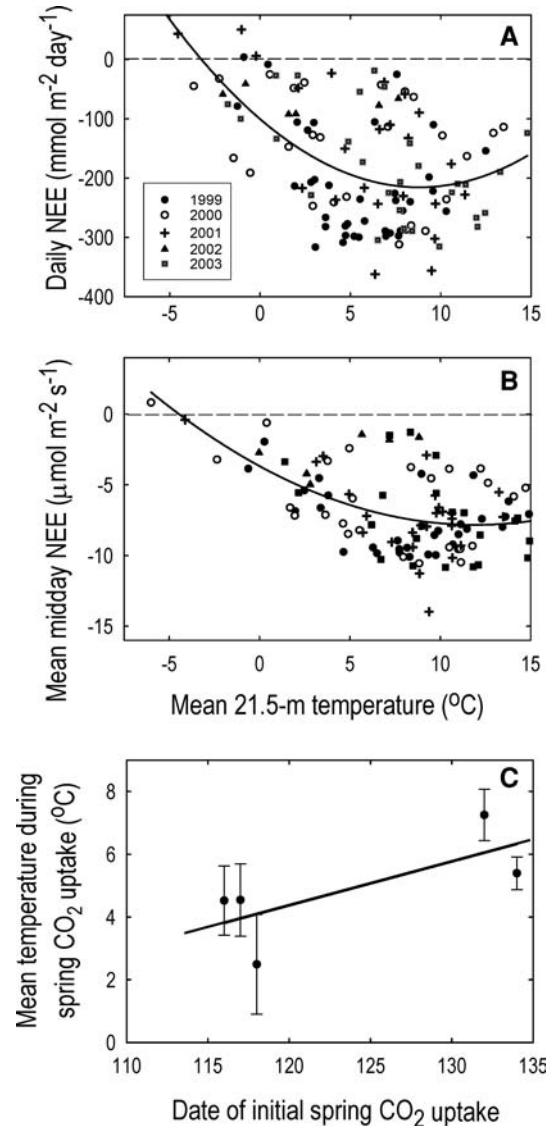


Fig. 3 a Daily NEE (NEE_{daily}) observed during the spring snow melt as a function of mean daily air temperature. Each point represents the value for 1 day. b Daytime mean of 30-min averaged (NEE_{30-min}) as a function of daytime mean air temperature (at 21.5 m) determined for the periods between 0800 h and 1600 h. c The mean daily temperature during the spring snow melt as a function of the date of initial springtime net CO_2 uptake. The initiation of spring net CO_2 uptake was determined as the first date NEE_{daily} was negative. Values represent the mean of all days within the snow melt period for each respective year \pm S.E. The line reflects the best-fit function as determined from linear regression analysis (see text for regression details)

probably became a net daily CO_2 source once again, before settling into a consistent pattern of continuous CO_2 uptake. Soil temperature climbed above $0^\circ C$ for the first time on DOY 86, well before the forest turn-on date, and remained slightly above zero through the snow melt period. In this year, the variable that most accurately predicted the forest turn-on date was the date of isothermality across the snow pack (i.e., the date when the temperature gradient across the vertical profile of the snow pack reached zero) (Fig. 4c). Soil moisture was

Table 2 Correlation between the average NEE_{30-min} and the average air temperature (measured at 21.5 m) during the period between 0800 h and 1600 h for three binned time periods: (1) the mid-winter period of January and February, (2) the period of 3 weeks immediately prior to the forest turn-on date, and (3) the combined days for the snowmelt period following the forest turn on date.

| Year | Mid-winter | 3-weeks before turn-on | Snowmelt after turn-on |
|------|--|---|--|
| 1999 | $y = -0.003x + 0.71$ $R^2 = 0.006$; $F = 0.26$; $P = 0.62$ T range = -14.2 to 3.5°C | $y = -0.23x + 0.35$ $R^2 = 0.84$; $F = 74.97$; $P < 10.000$ T range = -6.1 to 11.2°C | $y = -0.20x - 5.99$ $R^2 = 0.14$; $F = 4.80$; $P = 0.04$ T range = -0.6 to 14.9°C |
| 2000 | $y = -0.002x + 0.95$ $R^2 = 0.001$; $F = 0.046$; $P = 0.83^{***}$ T range = -15.5 to 4.0°C | $y = -0.16x + 0.06$ $R^2 = 0.20$; $F = 4.65$; $P = 0.04$ T range = -7.8 to 8.9°C | $y = -0.24x - 4.3$ $R^2 = 0.18$; $F = 5.18$; $P = 0.03^*$ T range = -6.0 to 15.1°C |
| 2001 | $y = -0.003x + 0.61$ $R^2 = 0.001$; $F = 0.09$; $P = 0.80^*$ T range = -14.5 to 5.4°C | $y = -0.19x - 0.60$ $R^2 = 0.43$; $F = 14.40$; $P = 0.001$ T range = -5.9 to 11.1°C | $y = -0.43x - 3.02$ $R^2 = 0.30$; $F = 9.87$; $P = 0.005$ T range = -4.1 to 13.7°C |
| 2002 | $y = -0.007x + 0.60$ $R^2 = 0.016$; $F = 0.73$; $P = 0.40^{**}$ T range = -15.8 to 5.5°C | $y = -0.19x - 0.20$ $R^2 = 0.23$; $F = 5.48$; $P = 0.03$ T range = -6.1 to 10.3°C | $y = 0.28x - 4.08$ $R^2 = 0.39$; $F = 2.60$; $P = 0.18$ T range = 0.0 to 8.8°C |
| 2003 | $y = -0.008x + 0.65$ $R^2 = 0.01$; $F = 0.54$; $P = 0.47$ T range = -19.6 to 7.4°C | $y = -0.27x - 0.53$ $R^2 = 0.28$; $F = 6.24$; $P = 0.02$ T range = -5.0 to 7.4°C | $y = -0.29x - 4.38$ $R^2 = 0.18$; $F = 5.01$; $P = 0.03$ T range = 1.4 to 18.0°C |

Regressions followed with * did not pass the test for normality of residuals at $P < 0.05$. Regressions followed with ** did not pass the test for constant variance at $P < 0.05$. Regressions followed with *** failed both tests simultaneously

observed to increase markedly immediately following the date of isothermality.

During the spring of 2002, air temperature fluctuated at a higher frequency and showed no distinct evidence of organized weather fronts, compared to the observations from 2001. We observed numerous isolated warm days in early spring with evidence of photosynthetic CO_2 uptake (Fig. 5d). For example, between DOY 90 and 100, air temperatures warmed each day above 5°C , correlating with a prolonged period of CO_2 uptake (marked by a in Figs. 5a, d). However, a short, but strong, cold period in the vicinity of DOY 107 caused reductions in CO_2 uptake to near zero (marked by b in Figs. 5a, d), and prevented the forest turn-on from being initialized until DOY 118. Soil temperatures were slower to reach 0°C in 2002, compared to 2001, probably due to the shallower snow pack and lower capacity for thermal insulation against freezing nights. Soil temperatures reached 0°C on approximately DOY 100, almost 3 weeks prior to the forest turn-on date. This was also the same approximate date that the snow pack became isothermal, and soil water content increased significantly (Figs. 5c, e). Thus, in this year, the potential for isothermality in the snow pack to trigger the forest turn-on was mitigated by cold air temperatures that settled over the site for several days. It is notable in Figs. 4 and 5 that ecosystem respiration rates did not increase during the spring snow melt. This trend is consistent with the data reported in Fig. 1, in which the average nighttime NEE_{30-min} (which solely reflects ecosystem respiration) increased by a factor of approximately 2, but the average daytime NEE_{30-min} (which reflects ecosystem respiration and gross photosynthesis) increased by a factor of approximately 10,

Only NEE measurements that did not include gap-filled data were used for this analysis. Linear regression models were used for all analyses. Statistically significant regressions are shown in bold type. T range refers to the total range in mean midday air temperature observed during each respective period

from mid-winter to the end of the spring snowmelt. These trends emphasize the fact that the dynamics in NEE during the snow melt are clearly driven by photosynthetic processes, not respiratory processes.

Branch and needle measurements of the recovery of CO_2 uptake capacity

In the first laboratory recovery experiment (conducted in the spring of 2000), we only made observations on lodgepole pine branches. Pre-dawn, field-measured needle Ψ_w were approximately -2.5 MPa, but changed after transport to the lab to approximately -1.1 MPa (Fig. 6); this was probably due to wood thawing and water re-equilibration in the branch system during transport. There was a time ($F = 25.09$; $df = 12,36$; $P < 0.05$), treatment ($F = 27.17$; $df = 2,6$; $P < 0.05$) and time-by-treatment interaction ($F = 10.65$; $df = 24,72$; $P < 0.05$) that described needle Ψ_w throughout the recovery experiment. In this experiment, we exposed the branches to three recovery treatments; high-light with hydration (HLH), low-light with hydration (LLH) and low-light dry (LLD). Needle Ψ_w increased as a function of time for the HLH and LLH treatments, reaching -0.3 MPa after 20 h. Branches in the LLD treatment showed increases in Ψ_w during the first few hours of recovery (probably due to warming of the wood tissues), followed by a sharp decrease to -4.5 MPa by 45 h post-harvest.

There was an effect of time ($F = 84.9$; $df = 12,36$; $P < 0.05$) in the recovery of intrinsic efficiency of PSII, as measured by F_v/F_m (Fig. 7a). Values increased from $F_v/F_m < 0.15$ (relative units) upon harvesting in the field, to $F_v/F_m = 0.50$ in 24 h and $F_v/F_m > 0.65$ after 40 h.

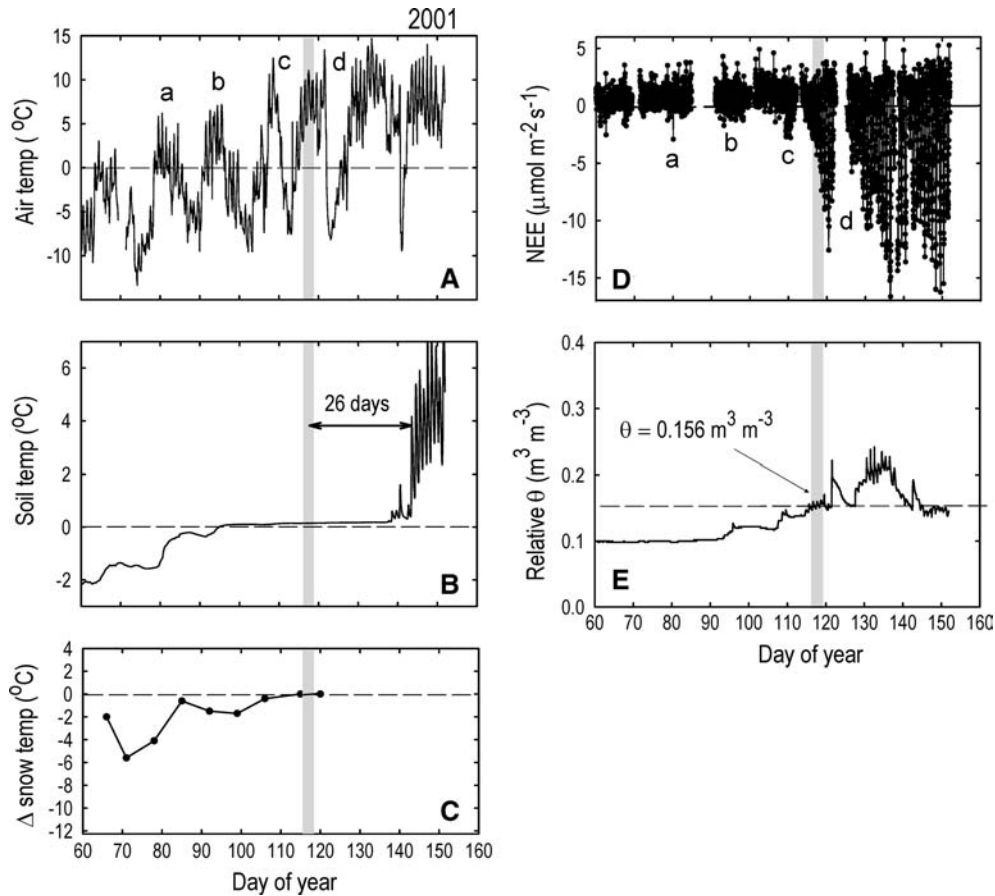


Fig. 4 Climatic variables and NEE for the period surrounding the springtime initiation of net CO₂ uptake during 2001. **a** Air temperature at 21.5 m on the eddy covariance tower. **b** Soil temperature at 10 cm depth (mean of three different thermocouples). The *arrow* indicates the 26-day period between the forest turn-on date and the date at which snow melt was completed. **c** Temperature gradient across the snow pack taken as the snow temperature measurement 10 cm below the upper surface of the snow pack and 10 cm above the lower surface of the snow pack.

d The 30-min averaged NEE measurement (no gap-filled data included) from the 21.5 m height on the eddy covariance tower. **e** Soil water content (measured as water volume relative to soil volume, θ) integrated across 15 cm soil depth (mean of three different probes). The value noted with the *arrow* in **e** represents the soil water content at the time of initiation of net CO₂ uptake. The *grey bar* represents the time of the forest turn-on (recovery of forest carbon uptake), and is represented in all panels for comparison purposes

There were no differences between treatments ($F=1.08$; $df=2,6$; $P<0.05$) and there was not an interaction between time and the different treatments ($F=0.76$; $df=24,72$; $P>0.05$). Thus, the only variable that was statistically related to the recovery of F_v/F_m was the increase in temperature. Induction of the xanthophyll cycle [(zeaxanthin + antheraxanthin)/(violaxanthin + antheraxanthin + zeaxanthin)] [hereafter referred to as $(Z+A)/(V+A+Z)$] decreased during the recovery treatments (Fig. 7b). At the onset of recovery, $(Z+A)/(V+Z+A)$ was greater than 0.8. Relative to the total pool of xanthophyll pigments, levels of $(Z+A)$ decreased through time in all treatments with the conversion state decreasing linearly to 0.27 for the LLH treatment, 0.35 for the HLH treatment, and to 0.55 for the LLD treatment. On the final day of measurement, the means of $(Z+A)/(V+Z+A)$ for the LLD and LLH treatments were significantly different ($F=0.05$; $df=3,2$; $P=0.048$), despite no significant differences in F_v/F_m .

Measurable stomatal conductance was observed on the first day of recovery in the HLH and LLH treatments, despite no measurable gas exchange in the field during the day prior to harvest (Fig. 8). During recovery of stomatal conductance, time and the interaction between time and the different recovery treatments were significant ($F=2.78$; $df=6,12$; $P<0.05$ and $F=2.57$; $df=12,24$; $P<0.05$, respectively). The HLH treatment consistently had higher conductance values ($0.51 \pm 0.20 \text{ mol m}^{-2} \text{ s}^{-1}$) compared to the LLH treatment ($0.22 \pm 0.09 \text{ mol m}^{-2} \text{ s}^{-1}$). Needles in both of these treatments exhibited stomatal conductances that were larger than those in the LLD treatment ($<0.035 \text{ mol m}^{-2} \text{ s}^{-1}$).

The A-Ci response of needles through time was dependent on recovery treatment ($F=29.9$; $df=12,74$; $P<0.01$). The LLD treatment did not produce a resolvable A-Ci curve during the experiment. The LLH and HLH treatments induced similar A-Ci responses

Fig. 5 Climatic variables and NEE for the period surrounding the springtime initiation of net CO₂ uptake during 2002. All panels are as described in Fig. 4

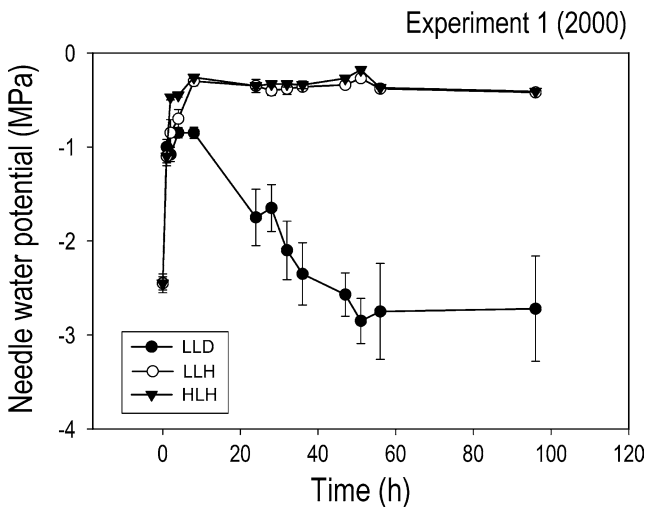
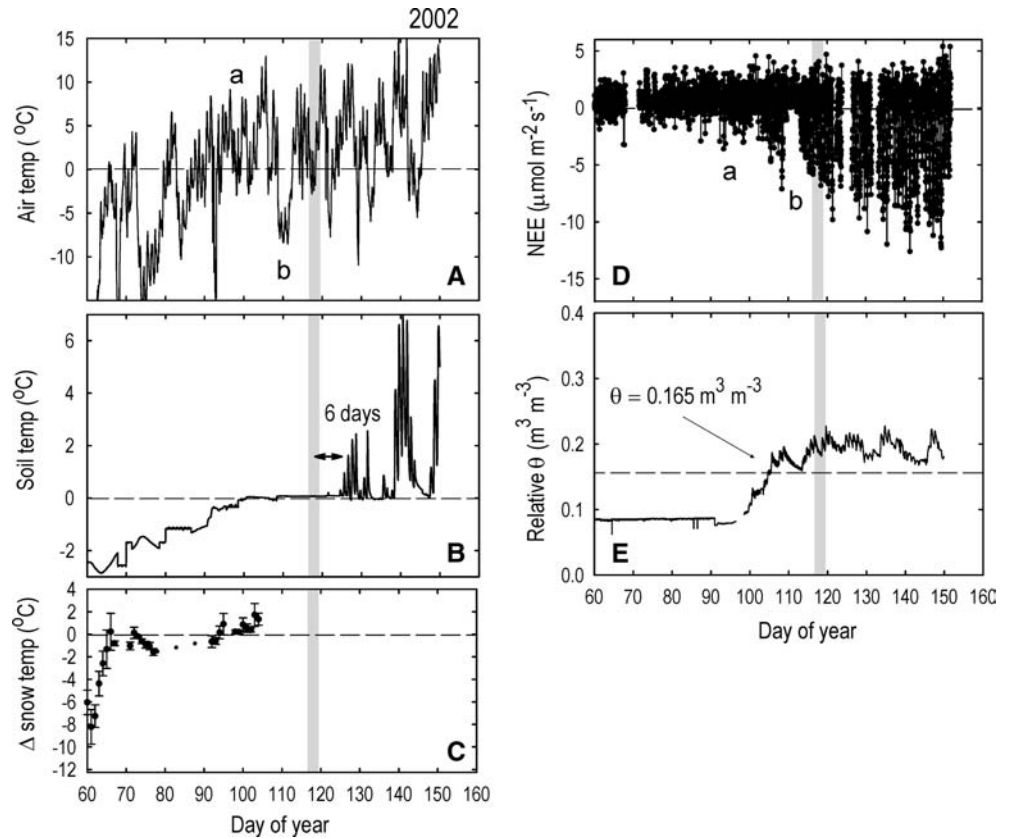


Fig. 6 Time-dependent changes in needle water potential during the recovery treatments of Experiment 1 on cut branches of lodgepole pine. Treatments are represented as low light, dry (LLD), low light hydrated (LLH), and high light, hydrated (HLH). Values represent the mean \pm SE ($n=3$ branches)

through time (Fig. 9). A single regression line described each of the time-points for these two treatments except for day 5 ($F=10.0$; $df=4,22$; $P<0.05$). On day 5, needles in HLH showed an initial slope that was steeper and a saturated region that was greater than the LLH

treatment. The maximum rate of carboxylation ($V_{C_{max}}$) increased from $10.3 \mu\text{mol m}^{-2} \text{s}^{-1}$ to $15.0 \mu\text{mol m}^{-2} \text{s}^{-1}$ from Day 2 to Day 3 in both hydration treatments (Table 3). By Day 5, that value had increased to $23.8 \mu\text{mol m}^{-2} \text{s}^{-1}$ in the HLH treatment compared to only $17.1 \mu\text{mol m}^{-2} \text{s}^{-1}$ in the LLH treatment. Neither dark respiration rate (R_d) nor triose phosphate utilization (TPU) limitation showed a trend over time; however, the maximum rate of whole-chain electron transport (J_{max}) increased from $32.6 \mu\text{mol m}^{-2} \text{s}^{-1}$ to greater than $60 \mu\text{mol m}^{-2} \text{s}^{-1}$ in the two treatments, and most of the increase occurred during the first 72 hours of the recovery treatments. The CO₂ compensation point (Γ) showed a decrease with time from 204 to $144 \mu\text{mol mol}^{-1}$ during the time from Day 2 to Day 3. By Day 5, Γ had not increased further in the HLH treatment, but had increased to $94 \mu\text{mol mol}^{-1}$ in the LLH treatment.

In the second experiment (conducted in the spring of 2004), we made observations on lodgepole pine and subalpine fir branches. Rather than focusing on the physiological mechanisms that control the recovery, in this experiment we aimed to determine whether differences exist in the recovery kinetics between these two species. From observations made during our previous experiment, we concluded that needles that are not hydrated during the recovery period do not exhibit recovery of photosynthetic CO₂ assimilation, even after 7 days, and despite the recovery of PSII efficiency. Thus,

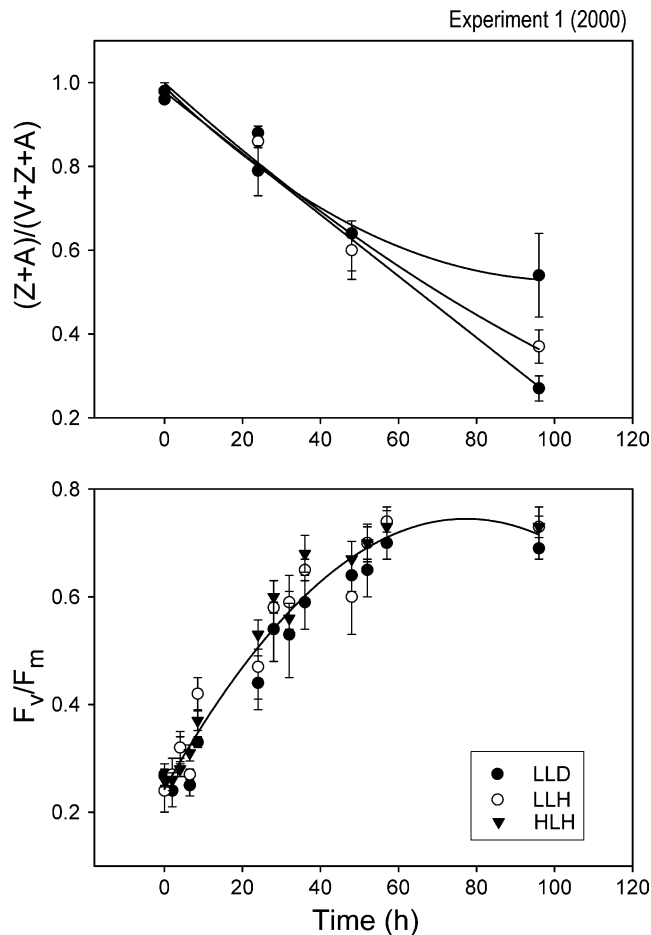


Fig. 7 Time-dependent changes in the ratio of xanthophyll cycle pigments (*upper panel*) and the intrinsic efficiency of photosystem II (F_v/F_m) (*lower panel*) for branches of lodgepole pine during Experiment 1. The lines represent “best-fit” regression plots obtained from either linear or second-order polynomial regression analyses. Values represent mean \pm SE ($n=3$ branches for the *upper panel* and 10 branches for the *lower panel*)

in this experiment, we focused on recovery in response to two hydration treatments, one in a warm temperature regime (WH) and one in a cold temperature regime (CH) and on two physiological measures that are least dependent on time-of-day and are easily measured in order to facilitate sequential sampling, chlorophyll fluorescence and CO_2 assimilation rate at normal ambient CO_2 concentration. In this case, the week prior to the harvesting of branches was characterized by warmer-than-normal temperatures at the field site. Perhaps in response to this warm period, the pre-dawn needle Ψ_w of lodgepole pine was already relatively high at the time of harvest. Time of hydration did not have a further effect in increasing the needle water potential of pines ($F=2.20$; $df=3,16$; $P=0.13$). Pre-dawn needle Ψ_w was relatively low in subalpine fir branches at the time of harvest (Table 4). Needle Ψ_w recovered after only 1 day of hydration in the WH regime, with time of hydration having a significant effect ($F=10.86$; $df=3,16$;

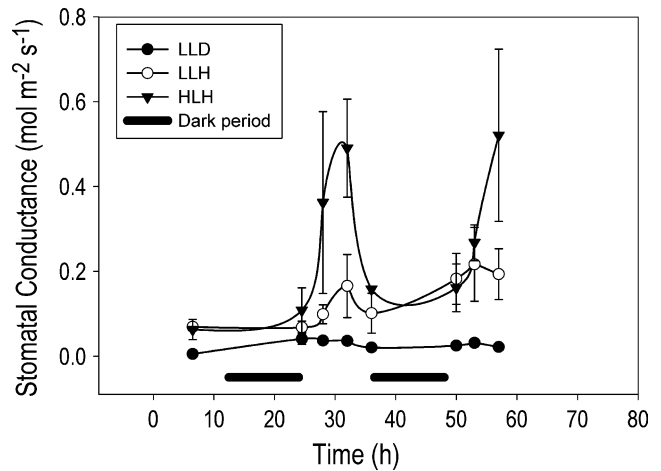


Fig. 8 Time-dependent changes in stomatal conductance to water vapor of lodgepole pine needles during Experiment 1. Stomatal conductance in this case is expressed on the basis of projected needle surface area, not total needle surface area. Treatment symbols are as described in Fig. 7. Values represent mean \pm SE ($n=5$ branches)

$P=0.0004$). In needles of subalpine fir, PSII photosynthetic efficiency was already relatively high at the time of collection (Day 0), despite relatively low needle Ψ_w (Table 4). This may have been a relict, remaining from some level of in situ photosynthetic recovery the previous week. In pine needles, PSII efficiency was still relatively low when needles were harvested, despite relatively high needle Ψ_w ; this might indicate the lack of photosynthetic recovery in this species the previous week, despite having experienced needle re-hydration. Within the first day in the WH treatment, PSII efficiencies in pine needles had increased to 93% of the observed maximum. In both species, there was a significant overall effect of time of hydration in the warm regime on recovery of F_v/F_m (subalpine fir, $F=84.88$; $df=4,36$; $P<0.0001$; lodgepole pine, $F=220.33$; $df=4,45$; $P<0.0001$) and significant ($P<0.05$) pairwise contrasts between Day 0 and all subsequent days, and Day 1 and all subsequent days. After Day 1, pairwise contrasts were not significant. In other words, in both species, recovery in F_v/F_m was complete after 1 day in the WH regime. At the time of harvest net CO_2 exchange of needles in both species solely reflected net CO_2 loss (Table 4). After 1 day in the WH treatment (indicated as “Day1” in Table 4), the needles of subalpine fir switched from net CO_2 loss to net CO_2 uptake, with CO_2 uptake rates being 34% of their eventual maximum. There was a significant effect of time of hydration on the recovery of CO_2 assimilation rate in subalpine fir ($F=18.70$; $df=4,25$; $P<0.0001$). Pine needles were considerably slower in their recovery in the WH treatment. Needles in lodgepole pine exhibited significant increases in net CO_2 uptake after 2 days of hydration, compared to 1 day in subalpine fir, and rates of CO_2 uptake significantly greater than 0 only after 7 days of recovery, compared

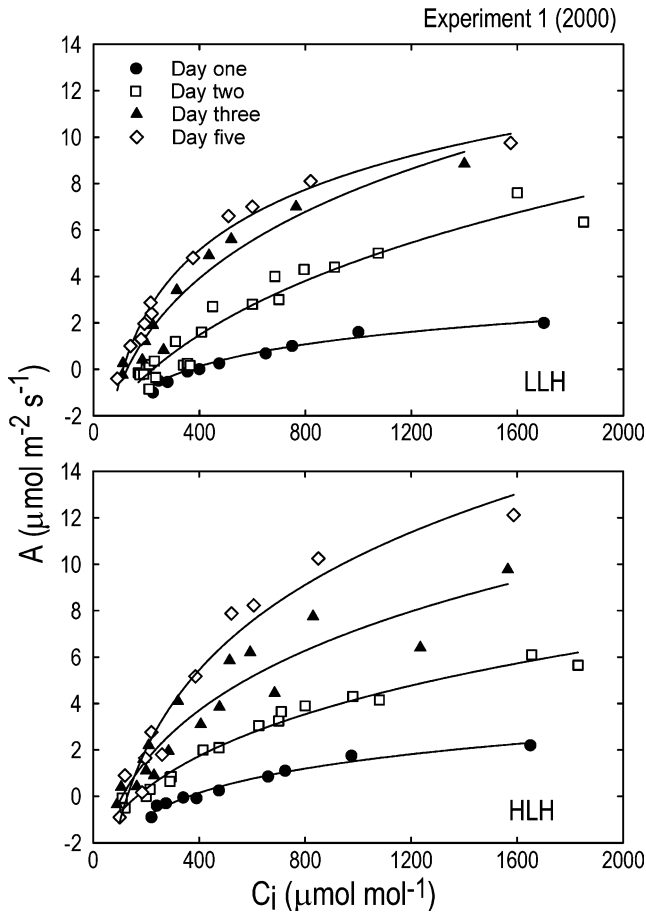


Fig. 9 Time-dependent recovery of the relationship between needle net CO₂ assimilation rate (A) and needle intercellular CO₂ concentration (C_i) in lodgepole pine during Experiment 1. Net CO₂ assimilation rate in this case is expressed on the basis of projected needle surface area, not total needle surface area. Treatment symbols are as described in Fig. 7. Each point represents one measurement. Lines were fitted to the points with “best-fit” second-order polynomials determined from regression analysis

to 1 day for subalpine fir. As we only sampled on days 3 and 7 in the recovery experiment, we conclude that pine needles require between 4 days and 7 days in a warm, hydrated state for significant photosynthetic recovery.

In the cold regime (CH), after 7 days of hydration, fir needles recovered to a significantly lower rate of net CO₂

uptake, compared to those in the WH regime (Table 4) (means compared between WH fir and CH fir significantly different; $t = 4.55$; 2-tailed $P = 0.004$), despite exhibiting similar needle Ψ_w values and photosystem II efficiencies. Needles of pine that were rehydrated in the cold regime did not regain the capacity for CO₂ uptake, even after 7 days, again despite having relatively high initial needle Ψ_w (means compared between WH pine and CH pine significantly different; $t = 5.50$; 2-tailed $P = 0.0005$). In pine needles, photosystem II efficiency (F_v/F_m) did not recover after 7 days in the CH treatment to the same level as that for needles in the WH treatment ($t = 15.58$; 2-tailed $P < 0.0001$).

Discussion

Considerable attention has recently been devoted to the timing of, and controls over, the springtime greening of deciduous forests (Goulden et al. 1996b; Bergh et al. 2003) and commencement of springtime photosynthetic activity in evergreen forests (Bergh and Linder 1999; Vaganov et al. 1999; Bergh et al. 2003; Suni et al. 2003; Tanja et al. 2003; Smith et al. 2004). Springtime CO₂ assimilation in northern hemisphere forests affects annual dynamics in the hemispheric CO₂ drawdown (Randerson et al. 1999) and is correlated with remotely-sensed patterns of surface ‘greening’ (Myneni et al. 1997; Way et al. 1997; Nichol et al. 2002). Evergreen forest trees in cold-winter climates normally downregulate photosynthetic activities during the winter and require warm weather cues to trigger recovery. The nature of these cues and the sequence of physiological responses involved in the recovery have been examined in the case of certain boreal forest species (e.g., Ensminger et al. 2004), but are largely uninvestigated for mid-latitude coniferous trees. In this study, we focused on a subalpine coniferous forest in the Rocky Mountains of Colorado. We demonstrated that (1) the time of recovery in the photosynthetic processes of the trees can be offset by several weeks from the time of recovery in the capacity of ecosystem carbon uptake, (2) once the capacity for carbon uptake does recover, CO₂ assimilation during the period of snow melt represents a significant, but variable component of growing-season NEE and annual NEE, (3) warm, early-spring, air temperatures are sufficient to

Table 3 Recovery of photosynthetic and respiratory variables for lodgepole pine in Experiment#1 in either the high light hydrated (HLH) or low light hydrated (LLH) treatments

| Treatment | Time of recovery (h) | R_d ($\mu\text{mol m}^{-2} \text{s}^{-1}$) | $V_{C_{\text{max}}}$ ($\mu\text{mol m}^{-2} \text{s}^{-1}$) | J_{max} ($\mu\text{mol m}^{-2} \text{s}^{-1}$) | Γ ($\mu\text{mol mol}^{-1}$) |
|-----------|----------------------|--|---|---|---------------------------------------|
| HLH | 48 | -2.11 | 10.3 | 38.9 | 205 |
| | 72 | -2.02 | 15.0 | 67.0 | 142 |
| | 120 | -3.25 | 23.8 | 69.5 | 144 |
| LLH | 48 | -2.85 | 12.7 | 50.3 | 224 |
| | 72 | -2.03 | 16.4 | 52.5 | 134 |
| | 120 | -1.21 | 17.1 | 48.5 | 94 |

Data represent the least squares regression estimations in the program Photosyn Assistant, for dark respiration rate (R_d), maximum carboxylation velocity of Rubisco ($V_{C_{\text{max}}}$), maximum rate of electron transport (J_{max}), and CO₂ compensation point (Γ)

Table 4 Needle water potential (Ψ_w), photosystem II efficiency (F_v/F_m), and net CO_2 assimilation rate at ambient CO_2 concentration (A) for needles of subalpine fir and lodgepole pine in Experiment#2 measured after varying times of recovery from winter photosynthetic downregulation in a warm or cold growth chamber with hydration of branches

| Variable | Subalpine fir | | | | | | | Lodgepole pine | | | | | | |
|--|--------------------|--------------------|--------------------|--------------------|-------------------|-----------------------|-----------------------|--------------------|----------------------|----------------------|-------------------|----------------------|--|--|
| | Day 0 (WH) | Day 1 (WH) | Day 2 (WH) | Day 3 (WH) | Day 7 (WH) | Day 7 (CH) | Day 0 (WH) | Day 1 (WH) | Day 2 (WH) | Day 3 (WH) | Day 7 (WH) | Day 7 (CH) | | |
| Needle Ψ_w (MPa) | -1.71 ± 0.60^a | -0.40 ± 0.08^b | -0.47 ± 0.02^b | -0.60 ± 0.04^b | ND | -0.83 ± 1.01^b | -0.68 ± 0.10^a | -0.59 ± 0.08^a | -0.73 ± 0.13^a | -0.41 ± 0.04^a | ND | -0.25 ± 0.05^a | | |
| F_v/F_m (rel units) | 0.58 ± 0.01^a | 0.73 ± 0.02^b | 0.77 ± 0.00^c | 0.80 ± 0.00^c | 0.78 ± 0.01^c | 0.68 ± 0.02^{abc} | 0.35 ± 0.02^{at} | 0.64 ± 0.01^b | 0.78 ± 0.01^c | 0.81 ± 0.01^c | 0.81 ± 0.01^c | 0.53 ± 0.02^{ab} | | |
| A ($\mu\text{mol m}^{-2} \text{s}^{-1}$) | -2.64 ± 1.16^a | 2.58 ± 0.63^b | 4.28 ± 0.80^b | 7.60 ± 0.38^c | 2.92 ± 1.38^b | 1.89 ± 0.39^{ab} | -2.61 ± 1.45^{ab} | -4.22 ± 1.00^a | 0.45 ± 0.33^{bc} | 0.39 ± 0.48^{bc} | 2.62 ± 0.70^c | -3.26 ± 0.81^a | | |

Values in the same row with the same letter are not significantly different at $P < 0.05$

Values represent the mean \pm SE ($n = 3-10$)

WH and CH represent warm, hydrated and cold, hydrated as described in the text. ND not determined

trigger limited photosynthetic recovery in NEE, but the availability of liquid soil water combined with even warmer air temperatures constitutes the set of environmental triggers that cause eventual full recovery in the capacity for ecosystem carbon uptake, (4) there is a specific sequence by which components of the photosynthetic apparatus recover and thus constrain the overall pattern and pace of recovery, and (5) differences exist in the rate of springtime recovery between the dominant tree species in this forest ecosystem, and probably the degree to which they respond to early spring versus late spring warming.

The springtime recovery of photosynthesis and carbon uptake in this forest represents a composite of responses extending across several weeks. It is difficult to assign a specific date to the recovery. Periodic and transient warm periods during the early spring trigger a limited capacity for photosynthetic CO_2 assimilation and reduce the rate of CO_2 loss from the forest, although this recovery is seldom strong enough to completely offset nighttime respiration and the daily CO_2 balance remains one of net loss. These early recovery events are characterized by multiple initiations and reversals depending on the passage of local weather systems. Later in the spring, after the snow pack becomes isothermal, snow melt begins and soil water availability increases, the forest is primed to a state whereby further warming can trigger a full recovery in forest photosynthetic capacity and high rates of carbon uptake return.

Over five consecutive years the fraction of $\text{NEE}_{\text{growing-season}}$, which was represented by $\text{NEE}_{\text{snow-melt}}$, ranged from 3 to 42% (Table 1). This variation could not be accounted for by differences in the time of autumn closure to the growing season, as this date varied little among the years. Interannual variation in $\text{NEE}_{\text{annual}}$ among several of the years can be better explained by interannual variation in $\text{NEE}_{\text{snow-melt}}$, than by interannual variation in $\text{NEE}_{\text{snow-free}}$. For example, in comparing the two extreme years with the highest (1999) and lowest (2002) $\text{NEE}_{\text{annual}}$, we observed that $\text{NEE}_{\text{snow-free}}$ was similar ($\Delta = 0.51 \text{ mol C m}^{-2}$) (Table 1). The difference in $\text{NEE}_{\text{snow-melt}}$ ($\Delta = 7.70 \text{ mol C m}^{-2}$), however, along with the difference in wintertime respiration ($\text{NEE}_{\text{winter}}$, $\Delta = -2.63 \text{ mol C m}^{-2}$), almost completely accounts for the difference in $\text{NEE}_{\text{annual}}$ ($\Delta = 5.58 \text{ mol C m}^{-2}$). As another example, we note the difference in $\text{NEE}_{\text{annual}}$ between the years 1999 and 2000. $\text{NEE}_{\text{snow-free}}$ was higher in 2000 by $2.42 \text{ mol C m}^{-2}$, compared to 1999, but $\text{NEE}_{\text{annual}}$ was lower by $1.91 \text{ mol C m}^{-2}$. The difference in $\text{NEE}_{\text{winter}}$ between these two years was only $0.19 \text{ mol C m}^{-2}$. The lower $\text{NEE}_{\text{annual}}$ in 2000, despite accumulating more carbon during the snow-free part of the growing season, can be accounted for by the difference in $\text{NEE}_{\text{snow-melt}}$.

We should add a note of explanation concerning our interpretation of the influence of $\text{NEE}_{\text{snow-melt}}$ on $\text{NEE}_{\text{growing-season}}$ and $\text{NEE}_{\text{annual}}$. The term $\text{NEE}_{\text{snow-melt}}$ is a hybrid composed of physiological and climatological

components. It is marked at the early-spring boundary by the time at which the trees recover physiologically and are able to use the snow-melt water, and at the late-spring boundary by the climatologically-determined end of the snow melt itself. Use of the melted snow water will no doubt continue for some time after the disappearance of the snow pack, although this cannot be determined solely by measurements of NEE and soil moisture. It would be informative to determine interannual variation in the parameter $NEE_{\text{snow-melt}}$ defined solely in physiological terms (i.e., with the late-spring boundary defined as the time when the trees cease using snow melt water). Studies are in progress to develop this insight using the stable isotope signatures of winter snow versus summer rain water. Nonetheless, the term $NEE_{\text{snow-melt}}$ does have inherent relevance to analyses of ecosystem carbon budgets. As defined in this study, $NEE_{\text{snow-melt}}$ represents the time between when the ecosystem begins to sequester carbon in the early spring and the time when the disappearance of snow in the late spring causes soil respiration rates to increase significantly (see Monson et al. 2002). Thus, this is the interval when the forest reaches its highest gross photosynthesis/respiration ratio, and thus its greatest potential to sequester carbon. Additionally, we note that as defined in this study $NEE_{\text{snow-melt}}$ reflects a conservative estimate of the influence of the snow melt period on interannual NEE dynamics. If anything, the contribution of $NEE_{\text{snow-melt}}$ to growing-season and annual NEE will increase once we know the actual extent of late-spring forest usage of snow-melt water.

During those years when the forest turn-on occurred earlier in the spring, $NEE_{\text{snow-melt}}$ and NEE_{annual} were lowest (Fig. 2, Table 1). This relationship was due to two effects. First, we observed a springtime temperature dependence of NEE reflecting a low temperature constraint during the earliest part of the recovery (Fig. 3); this result is consistent with the statistical path analysis conducted by Huxman et al. (2003), which showed that cooler spring periods have a negative influence on NEE. Second, during those years with earlier springs the depth of the snow pack at the forest turn-on date was lower; thus, earlier springs coincided with less snowmelt water to drive CO_2 uptake. One hypothesis that does not receive support from our observations concerns the question of whether an early spring with a low snow pack influences NEE during the subsequent snow-free part of the growing season; in other words, does less snow in the spring lead to a stronger moisture constraint the following summer? The anecdotal evidence from our study does not support this hypothesis. For example, the spring snow packs of 1999 and 2002 reflected the high and low extremes observed during our study, yet NEE during the snow-free periods of these two years were nearly equal. It is likely that summer rains have greater control over summertime NEE than snow water from the previous spring. There is clearly room for further research into the coupling between spring and summer hydrological regimes and their influence on NEE.

Our conclusion that earlier springs are correlated with lower rates of annual NEE has important ramifications for predicting the effects of future climate change on the terrestrial carbon cycle. In general, earlier spring warming is predicted to enhance forest NPP, especially in sites with cold winter climates (White et al. 1999; Arain et al. 2002; Bergh et al. 2003). In deciduous forest ecosystems of the eastern U.S. and southern Canada, earlier springs were correlated with higher annual rates of carbon uptake (Goulden et al. 1996b; Black et al. 2000; Barr et al. 2002). In a deciduous forest ecosystem, annual CO_2 uptake is highly constrained by the fraction of the growing season during which newly-formed leaves are expanding and forest leaf-area index (LAI) is below its seasonal maximum; normally, an earlier spring reduces this fraction and increases the time during which the forest can assimilate CO_2 at its maximum LAI. In an evergreen forest the seasonal constraint on CO_2 uptake caused by LAI is small compared to the various environmental constraints that affect NEE, particularly those associated with temperature and moisture. In an evergreen forest, an earlier spring will only have a positive influence on annual NEE if these additional constraints are relieved; a condition that we did not observe during our 5 years of observations.

The environmental triggers that facilitate the switch from a winter phase of net CO_2 loss to a spring phase of net CO_2 gain include both isothermality of the snow pack and the occurrence of favorable air temperatures. Although we observed multiple initiations and reversals of CO_2 uptake in the $NEE_{30\text{-min}}$ data depending on the passage of local warm and cold weather systems (Figs. 4 and 5), we never observed consistent cumulative daily CO_2 uptake prior to isothermality in the snow pack. In studies of photosynthetic recovery in boreal forest conifers, Ensminger et al. (2004) observed similar dynamics with regard to reversible stretches of warm weather and its influence on PSII activity. In an examination of five boreal forest sites, Tanja et al. (2003) found a strong correlation between the forest turn-on date and the mean air temperature during the few days preceding the date (also see Hadley and Schedlbauer 2002; Suni et al. 2003). Thus, there is broad support for the role of air temperature in controlling some level of recovery in the photosynthetic systems of the forest. There is less support for the role of soil moisture. In the studies of Tanja et al. (2003) soil moisture availability was poorly correlated with the forest turn-on date. Clearly, there are differences in the nature of the environmental triggers between high-latitude boreal forests where seasonal thaw of the permafrost occurs well into the growing season and lower latitude subalpine forests where there is no permafrost.

The downregulation of photosynthesis in evergreen conifers during the winter months has been attributed to low temperature induced photoinhibition of PSII (Öquist and Huner 2003; Yamazaki et al. 2003). However, studies to date have not simultaneously considered recovery in the photochemical, diffusive and

carboxylation components of the photosynthetic apparatus. We argue that only by considering the responses of all of the primary components of the photosynthetic apparatus, can we build a complete understanding of springtime recovery. Our studies showed that recovery of photosynthesis from wintertime downregulation occurred in a series of events involving all of these physiological processes. Recovery of stomatal conductance (g_s) and the intrinsic efficiency of PSII (F_v/F_m) occurred rapidly and in parallel (Figs. 7 and 8). F_v/F_m has been documented to achieve near-full recovery in less than 70 h for conifer species in response to an increase in temperature (Verhoeven et al. 1998). In the present study, recovery in lodgepole pine was even faster, recovering to near-maximal values within 48 h. Furthermore, the recovery of F_v/F_m in lodgepole pine needles was not dependent on needle Ψ_w , only warm temperature, as has been shown previously (Ensminger et al. 2004). In contrast to the pattern for F_v/F_m , $(Z+A)/(V+Z+A)$ was dependent on needle Ψ_w , in addition to temperature (Fig. 7). Perhaps due to these different responses, PSII recovery and the xanthophyll cycle did not show concurrent recovery in all cases, as has been seen in *Pinus ponderosa* and *Pseudotsuga menziesii* (Verhoeven et al. 1996). In our study, the well described relationship between PSII efficiency and $(Z+A)$ pools was observed in all cases except the non-hydrated recovery treatment. Although it remains uncertain why the reconversion of $Z+A$ to V was incomplete in this case, several recent studies have shown that additional photosynthetic proteins (PsbS for example; see Li et al. 2000) are important for zeaxanthin-dependent energy quenching; this further complicates the relationship between PSII efficiency and $Z+A$ pools (also see Adams et al. 2001). Given the potential for multiple factors to influence the coupling between PSII recovery and $Z+A$ pool size, it is possible that the springtime recovery of PSII function occurs despite the existence of high $Z+A$ pools under some conditions.

The recovery of photosynthetic carboxylation capacity occurred at the slowest rate of those processes that we studied, as evidenced by the slow recovery of the initial slope of the $A:C_i$ response (Fig. 9). We did not observe recovery of the $A:C_i$ relationship in needles kept in the LLD treatment. The maximum carboxylation rate of Rubisco ($V_{C_{max}}$) reached a maximum in the HLH treatment as compared to the LLH treatment (Table 3), suggesting that in addition to water, light is important for the upregulation of Rubisco activity. The slow pace at which $V_{C_{max}}$ was up-regulated and its reliance on several environmental variables suggests that recovery from winter downregulation requires not only changes in the activation state of Rubisco, but also de novo synthesis of Rubisco protein. The recovery of $V_{C_{max}}$ occurred at a different rate than that for whole-chain electron transport, as reflected in the estimated J_{max} , suggesting a lack of biochemical coordination between these two processes during springtime up-regulation.

When all processes are considered within a sequential context, it appears as though photosynthetic recovery is (1) initiated by response to warm air temperatures through the inductive up-regulation of PSII caused in part by disengagement of thermal energy dissipation by zeaxanthin and in part by the upregulation of whole-chain electron transport rate, (2) continued during soil warming as water is provided to the hydraulic system and the stomata begin to exhibit greater amplitude in their diurnal dynamics, and (3) completed as Rubisco enzyme is reactivated, re-synthesized, and/or re-allocated from storage pools to provide recovery of the carboxylation potential of the chloroplasts. Recovery of maximal springtime rates of forest net CO_2 uptake appears to occur only after all three of these stages are completed.

We observed interspecific differences in the timing of photosynthetic recovery. Subalpine fir needles recovered near-maximal photosynthetic capacities within 3 days after being rehydrated at a warmer temperature (Table 4). Needles of lodgepole pine required at least 4 days, and perhaps as many as 7 days, for photosynthetic recovery. The ecological and adaptive reasons for these differences are not clear at the current time. However, in general, pines tend to occupy drier habitats compared to firs (Rebertus et al. 1991; DeLucia et al. 2000; Martinez-Vilalta et al. 2004). It might be that the suite of photosynthetic adaptations that facilitate drought tolerance in pines, includes a slow, generally conservative response to transitions from dry to wet conditions. The differential responses of fir and pine may explain our observation of limited photosynthetic recovery early in the spring, with a full recovery in carbon uptake occurring much later. Rapid but partial photosynthetic recovery of fir trees in response to transient warm periods, and concomitant partial thawing of water in the branches and bole, may explain the weak signal in forest CO_2 uptake that we observed early in the spring. Recovery of pine may require the initiation of snow melt and longer, sustained periods of warm air temperature, such as occur later in the spring. A research investigation into the in situ patterns of photosynthetic recovery during the early and late spring in these two species, as well as the third important species, Engelmann spruce, is clearly justified.

Our results show that the timing of the transition between wintertime down regulation and springtime upregulation of net CO_2 uptake has an important role in controlling the rate of annual forest carbon uptake in this subalpine, coniferous forest. This conclusion is consistent with the many other past reports that earlier springs have a significant effect on annual NEE in forest ecosystems. However, from these past studies, we conclude that it is more rare to observe a negative influence of an early spring on annual NEE, as we have shown here, than a positive influence. The issue as to whether future climate warming, and concomitantly earlier springs, will enhance CO_2 uptake in cold-climate forests should continue to be viewed as unresolved. The envi-

ronmental triggers that control the transition from winter net CO₂ loss to spring net CO₂ gain appear to be consistent at both the needle and ecosystem scales; i.e., both liquid water and warm air temperatures are required for recovery at both scales. With a deeper understanding of how specific physiological and biochemical processes interact with these triggers, we should be able to improve our predictions of how future climate change, and particularly the onset of earlier springs, will influence ecosystem, and even global, dynamics in surface-atmosphere carbon exchange. The development of these predictions will likely require different approaches for deciduous and evergreen, coniferous forests. However, given that there are discernable mechanistic controls, that these mechanisms tightly couple springtime NEE to the prevailing environment, and that these mechanisms appear to be consistent across scales of observation, the problem of prediction is a tractable one.

Acknowledgements We are grateful for the research contributions of many students and colleagues, including Kimberley Sparks, Bill Baugh, Dr. Chuixiang Yi, Sarah Schliemann, Andy McNow, Nathan Monson, Greg Monson, John Munch, Thomas Zukowski, and Wumesh Khatri. We are grateful to Mark Williams, Mark Loesleben and Andy O'Reilly who provided valuable guidance to making the snow temperature measurements. We thank Dr. Bill Bowman (University of Colorado Mountain Research Station) for providing valued logistical support in establishing and maintaining the Niwot Ridge AmeriFlux site and access to an additional gas exchange system. We thank Gordon Maclean and Tony Delany (National Center for Atmospheric Research) for their long-standing commitment to help with all types of technical issues surrounding the instrumentation at the Niwot Ridge AmeriFlux tower. We thank Dr. William Adams and Barbara Demmig-Adams for providing valuable access to the HPLC system used in the pigment analysis and to the chlorophyll fluorescence system used in the first recovery experiment. This work was financially supported by a grant from the South Central Section of the National Institute for Global Environmental Change (NIGEC) through the US Department of Energy (BER Program) (Cooperative Agreement No. DE-FC03-90ER61010). Any opinions, findings and conclusions or recommendations expressed in this publication are those of the authors and do not necessarily reflect the views of the DOE.

References

- Adams WW, Demmig-Adams B (1992) Operation of the xanthophyll cycle in higher plants in response to diurnal changes in incident sunlight. *Planta* 189:390–398
- Adams WW, Demmig-Adams B, Rosenstiel TN, Ebbert V (2001) Dependence of photosynthesis and energy dissipation activity upon growth form and light environment during the winter. *Photosyn Res* 67:51–62
- Arain MA, Black TA, Barr AG, Jarvis PG, Massheder JM, Verseghy DL, Nesci Z (2002) Effects of seasonal and interannual climate variability on net ecosystem productivity of boreal deciduous and conifer forests. *Can J For Res* 32:878–891
- Baldocchi DD (2003) Assessing the eddy covariance technique for evaluating carbon dioxide exchange rates of ecosystems: past, present and future. *Global Change Biol* 9:479–492
- Barr AG, Griffis TJ, Black TA, Lee X, Staebler RM, Fuentes JD, Chen Z, Morgenstern K (2002) Comparing the carbon budgets of boreal and temperate deciduous forest stands. *Can J For Res* 5:813–822
- Bergh J, Linder S (1999) Effects of soil warming during spring on photosynthetic recovery in boreal Norway spruce stands. *Global Change Biol* 5:245–253
- Bergh J, Freeman M, Sigurdsson B, Kellomaki S, Laitinen K, Niinisto S, Peltola H, Linder S (2003) Modelling the short-term effects of climate change on the productivity of selected tree species in Nordic countries. *For Ecol Manag* 183:327–340
- Black TA, Chen WJ, Barr AG, Arain MA, Chen Z, Nesci Z, Hogg EH, Neumann HH, Yang PC (2000) Increased carbon sequestration by a boreal deciduous forest in years with a warm spring. *Geophys Res Lett* 27:1271–1274
- Chen JM, Rich PM, Gower ST, Norman JM, Plummer S (1997) Leaf area index of boreal forests: Theory, techniques and measurements. *J Geophys Res* 102:29429–29443
- Day TA, DeLucia EH, Smith WK (1989) Influence of cold soil and snowcover on photosynthesis and leaf conductance in two Rocky Mountain Conifers. *Oecologia* 80:546–552
- DeLucia EH, Maherali H, Carey EV (2000) Climate-driven changes in biomass allocation in pines. *Global Change Biol* 6:587–593
- Demmig-Adams B, Adams W, Barker DH, Logan BA, Verhoeven AS, Bowling DR (1996) Using chlorophyll fluorescence to assess the allocation of absorbed light to thermal dissipation of excess excitation. *Physiol Plant* 98:253–264
- Ensminger I, Sveshnikov D, Campbell DA, Funk C, Jansson S, Lloyd J, Shibistova O, Oquist G (2004) Intermittent low temperatures constrain spring recovery of photosynthesis in boreal Scots pine forests. *Global Change Biol* 10:995–1008
- Gilmore AM, Yamamoto HY (1991) Resolution of lutein and zexanthin using a nonendcapped, lightly carbon-loaded C18 high-performance liquid chromatographic column. *J Chrom* 543:137–145
- Goulden ML, Munger JW, Fan S-M, Daube BC, Wofsy SC (1996a) Measurements of carbon sequestration by long-term eddy covariance: Methods and a critical evaluation of accuracy. *Global Change Biol* 2:169–182
- Goulden ML, Munger JW, Fan S-M, Daube BC, Wofsy SC (1996b) CO₂ exchange by a deciduous forest: response to interannual climate variability. *Science* 271:1576–1578
- Hadley JL, Schedlbauer JL (2002) Carbon exchange of an old-growth eastern hemlock (*Tsuga canadensis*) forest in central New England. *Tree Physiol* 22:1079–1092
- Harley PC, Thomas RB, Reynolds JF, Strain BR (1992) Modelling photosynthesis of cotton grown in elevated CO₂. *Plant, Cell & Environ* 15:271–282
- Huxman TE, Hamerlynck EP, Moore BD, Smith SD, Jordan DN, Zitzer SF, Nowak RS, Coleman J, Seemann JR (1998) Photosynthetic down-regulation in *Larrea tridentata* exposed to elevated atmospheric CO₂: interaction with drought under glasshouse and field (FACE) exposure. *Plant, Cell & Environ* 21:1153–1161
- Huxman TE, Turnipseed AA, Sparks JP, Harley PC, Monson RK (2003) Temperature as a control over ecosystem CO₂ fluxes in a high-elevation, subalpine forest. *Oecologia* 134:537–546
- Jacob J, Greitner C, Drake BG (1995) Acclimation of photosynthesis in relation to Rubisco and non-structural carbohydrate contents and in situ carboxylase activity in *Scirpus olneyi* grown at elevated CO₂ in the field. *Plant, Cell & Environ* 18:875–884
- Jurik TW, Briggs GM, Gates DM (1988) Springtime recovery of photosynthetic activity of white pine in Michigan. *Can J Bot* 66:138–141
- Kaimal JC, Finnigan JJ (1994) Atmospheric boundary layer flows: their structure and measurement. Oxford University Press, Oxford
- Law BE, Williams M, Anthoni PM, Baldocchi DD, Unsworth MH (2000) Measuring and modelling seasonal variation of carbon dioxide and water vapour exchange of a *Pinus ponderosa* forest subject to soil water deficit. *Global Change Biol* 6:613–630

- Leverenz JW, Öquist G (1987) Quantum yields of photosynthesis at temperatures between 2 degrees and 35 degrees C in a cold-tolerant C₃ plant (*Pinus sylvestris*) during the course of one year. *Plant Cell Environ* 10:287–295
- Li S-P, Björkman O, Shih C, Grossman AR, Rosenquist M, Jansson S, Niyogi KK (2000) A pigment-binding protein essential for regulation of photosynthetic light harvesting. *Nature* 403:391–395
- Lloyd J, Langenfelds RL, Francey RJ, Gloor M, Tchebakova NM, Zolotoukhine D, Brand WA, Werner RA, Jordan A, Allison CA, Zrazhewske V, Shibistova O, Schulze ED (2002) A trace-gas climatology above Zotino, central Siberia. *Tellus (Ser B)* 54:749–767
- Lundmark T, Bergh J, Strand M, Koppel A (1998) Seasonal variation of maximum photochemical efficiency in boreal Norway spruce stands. *TREES-Struc Func* 13:63–67
- Martinez-Vilalta J, Sala A, Pinol J (2004) The hydraulic architecture of Pinaceae—a review. *Plant Ecol* 171:3–13
- Monson RK, Turnipseed AA, Sparks JP, Harley PC, Scott-Denton LE, Sparks K, Huxman TE (2002) Carbon sequestration in a high-elevation, subalpine forest. *Global Change Biol* 8:459–478
- Myneni RB, Keeling CD, Tucker CJ, Asrar G, Nemani RR (1997) Increased plant growth in the northern high latitudes from 1981 to 1991. *Nature* 386:698–702
- Nichol CJ, Lloyd J, Shibistova O, Arneth A, Roser C, Knohl A, Matsubara S, Grace J (2002) Remote sensing of photosynthetic-light-use efficiency of a Siberian boreal forest. *Tellus (Ser B)* 54:677–687
- Öquist G, Huner NPA (2003) Photosynthesis of overwintering evergreen plants. *Ann Rev Plant Biol* 54:329–355
- Ottander C, Öquist G (1991) Recovery of photosynthesis in winter-stressed Scots pine. *Plant, Cell Environ* 14:345–349
- Pedhazur EJ (1997) Multiple regression in behavioral research, 3rd edn. Harcourt Brace College Publishers, New York
- Potvin C, Lechowicz MJ, Tardif S (1990) The statistical analysis of ecophysiological response curves obtained from experiments involving repeated measures. *Ecology* 71:1389–1400
- Randerson JT, Field CB, Fung IY, Tans PP (1999) Increases in early season ecosystem uptake explain recent changes in the seasonal cycle of atmospheric CO₂ at high northern latitudes. *J Geophys Res* 26:2765–2768
- Rebertus AJ, Burns BR, Veblen TT (1991) Stand dynamics of *Pinus flexilis*-dominated sub-alpine forests in the Colorado Front Range. *J Veg Sci* 2:445–458
- Smith WK (1985) Environmental limitations on leaf conductance in central Rocky Mountain conifers, USA. In: Turner H, Tranquillini W (eds) Establishment and tending of subalpine forest: research and management. *Eidg Anst Forstl Versuchsw Ber* 270, pp 95–101
- Smith NV, Saatchi SS, Randerson JT (2004) Trends in high northern latitude soil freeze and thaw cycles from 1988 to 2002. *J Geophys Res* 109:Art. No. D12101
- Suni T, Berninger F, Markkanen T, Keronen P, Rannik U, Vesala T (2003) Interannual variability and timing of growing-season CO₂ exchange in a boreal forest. *J Geophys Res* 108(D9):Art No. 4265
- Tanja S, Berninger F, Vesala T, Markkanen T, Hari P, Makela A, Ilvesniemi H, Hanninen H, Nikinmaa E, Huttula T, Laurila T, Aurela M, Grelle A, Lindroth A, Arneth A, Shibistova O, Lloyd J (2003) Air temperature triggers the recovery of evergreen boreal forest photosynthesis in spring. *Global Change Biol* 9:1410–1426
- Troeng E, Linder S (1982) Gas-exchange in a 20-year old stand of Scots pine. 1. Net photosynthesis of current and one-year old shoots within and between seasons. *Physiol Plant* 54:7–14
- Turnipseed AA, Blanken PD, Anderson DE, Monson RK (2002) Energy budget above a high-elevation subalpine forest in complex topography. *Agric For Meteorol* 110:177–201
- Turnipseed AA, Anderson DE, Blanken PD, Baugh WM, Monson RK (2003) Airflows and turbulent flux measurements in mountainous terrain Part 1. Canopy and local effects. *Agric For Meteorol* 119:1–21
- Turnipseed AA, Anderson DE, Blanken PD, Burns S, Monson RK (2004) Airflows and turbulent flux measurements in mountainous terrain Part 2. Mesoscale effects. *Agric For Meteorol* (in press)
- Vaganov EA, Hughes MK, Kirilyanov AV, Schweingruber FH, Silkin PP (1999) Influence of snowfall and melt timing on tree growth in subarctic Eurasia. *Nature* 400:149–151
- Verhoeven AS, Adams WW, Demmig-Adams B (1996) Close relationship between the state of the xanthophyll cycle pigments and photosystem II efficiency during recovery from winter stress. *Physiol Plant* 96:567–576
- Verhoeven AS, Adams WW, Demmig-Adams B (1998) Two forms of sustained xanthophyll cycle-independent energy dissipation in overwintering *Euonymus kiautschovicus*. *Plant Cell Environ* 21:893–903
- Verhoeven AS, Adams WW, Demmig-Adams B (1999) The xanthophyll cycle and acclimation of *Pinus ponderosa* and *Malva neglecta* to winter stress. *Oecologia* 118:277–287
- Way J, Zimmermann R, Rignot E, McDonald K, Oren R (1997) Winter and spring thaw as observed with imaging radar at BOREAS. *J Geophys Res* 102:29673–29684
- Webb EK, Pearman GI, Leuning R (1980) Correction of flux measurements for density effects due to heat and water vapor transfer. *Quart J Roy Meteorol Soc* 106:85–100
- White MA, Running SW, Thornton PE (1999) The impact of growing-season length variability on carbon assimilation and evapotranspiration over 88 years in the eastern US deciduous forest. *Intl J Biometeorol* 42:139–145
- Wilczak JM, Oncley SP, Stage SA (2001) Sonic anemometer tilt correction algorithms. *Bound Lay Meteor* 99:127–150
- Yamazaki J, Ohashi A, Hashimoto Y, Negishi E, Kumagai S, Kubo T, Oikawa T, Maruta E, Kamimura Y (2003) Effects of high light and low temperature during harsh winter on needle photodamage of *Abies mariesii* growing at the forest limit on Mt. Norikura in Central Japan. *Plant Sci* 165:257–264